Langmuir
Article
pubs.acs.org/Langmuir

One-Step Preparation of Regular Micropearl Arrays for Two-Direction Controllable Anisotropic Wetting

Si-Zhu Wu,[†] Dong Wu,[†] Jia Yao,[†] Qi-Dai Chen,*[,†] Jian-Nan Wang,[†] Li-Gang Niu,[†] Hong-Hua Fang,[†] and Hong-Bo Sun*[,†,‡]

[†]*State Key Laboratory on Integrated Optoelectronics, College of Electronic Science and Engineering, Jilin University, 2699 Qianjin Street, Changchun 130012, China, and* [‡]*College of Physics, Jilin University, 119 Jiefang Road, Changchun 130023, China*

Received April 20, 2010. Revised Manuscript Received May 12, 2010

In this paper, one simple method to control two-direction anisotropic wetting by regular micropearl arrays was demonstrated. Various micropearl arrays with large area were rapidly fabricated by a kind of improved laser interference lithography. Specially, we found that the parallel contact angle (CA) θ_2 decreased from 93° to 67° as the intensity ratio of four laser beams increased from 2:1 to 30:1, while the perpendicular CA θ_1 determined by the thickness of the resin remained constant. This was interpreted as the decrease of height variations Δh from 1100 to 200 nm along the parallel direction caused by the increase of the intensity ratio. According to this rule, both θ_1 and θ_2 could be simultaneously controlled by adjusting the height variation Δh and the resin thickness. Moreover, by combining appropriate design and low surface energy modification, a natural anisotropic rice leaf exhibiting CAs of 146° ± 2°/153° ± 3° could be mimicked by our anisotropic biosurface with the CAs 145° ± 1°/150° ± 2°. We believe that these controlled anisotropic biosurfaces will be helpful for designing smart, fluid-controllable interfaces that may be applied in novel microfluidic devices, evaporation-driven micro/nanostructures, and liquid microdroplet directional transfer.

Introduction

The study of natural special surfaces and design of artificial functional biomimetic surfaces have become a hot topic due to various useful functions, such as the self-cleaning of the lotus leaf,[1] the iridescence of the butterfly wing,[2] the antireflection of the moth eye,[3] and the anisotropy of the rice leaf.[4] Research showed that surface micro/nanostructures were the key factor for these special functions. Various biomimetic surfaces with superhydrophobicity,[5−9] structural colors,[10,11] or antireflection[12,13] capability have been realized by preparing different microstructures. Biomimetic anisotropic surfaces also have been widely studied due to their important applications in microfluidic devices,[14,15] evaporation-driven nanopatterns,[16,17] and liquid pumps.[18] Many techniques such as photolithography,[19,20] surface wrinking,[21] electrospinning,[22] and interference lithography[17,23,24] have been developed to realize anisotropic wetting on groove microstructures. For example, Morita et al.[19] reported macroscopic wetting anisotropy on the line-patterned surface of a fluoroalkylsilane monolayer by vacuum ultraviolet photolithography; Zhao et al.[23] realized weak anisotropic wetting characteristics on a submicrometer-scale periodic grooved surface on azobenzene-containing multiarm star polymer films by laser interference; Sommers and Jacobi[20] achieved anisotropic wettability on an aluminum surface by standard photolithographic technique; Chung et al.[21] reported anisotropic wetting on microwrinkled surfaces; Sun et al.[24] found strong dependence between the anisotropy and the groove height and realized controllable anisotropy along one direction.[22] Although great progress has been made, these works focused on single level parallel grooved structures, whose applications were limited because only the perpendicular contact angle (CA) of grooves could be controlled. The parallel CA of grooves was determined by the groove materials and could not be freely designed because there are no height variations along this direction. Most of the parallel CAs are very low (∼60°).[17,19−24] Even after low surface energy modification, the maximal parallel CA on groove structures was about 126°,[25] far smaller than the one (∼150°) of natural anisotropic surfaces. Compared with a single direction, two directional controls were highly desirable and would find broader applications in high-performance functional

*To whom correspondence should be addressed. E-mail: hbsun@jlu.edu.cn (H.-B.S.); chenqd@jlu.edu.cn (Q.-D.C.). Homepage: http://www.lasun-jlu.cn/.

(1) Neinhuis, C.; Barthlott, W. *Ann. Bot.* **1997**, *79*, 667.
(2) Sato, O.; Kubo, S.; Gu, Z. Z. *Acc. Chem. Res.* **2009**, *42*, 1.
(3) Bernhard, C. G. *Endeavour* **1967**, *99*, 1935.
(4) Feng, L.; Li, S. H.; Li, Y. S.; Li, H. J.; Zhang, L. J.; Zhai, J.; Song, Y. L.; Liu, B. Q.; Jiang, L.; Zhu, D. B. *Adv. Mater.* **2002**, *14*, 1857.
(5) Yu, X.; Wang, Z.; Jiang, Y.; Shi, F.; Zhang, X. *Adv. Mater.* **2005**, *17*, 1289.
(6) Xu, L.; Chen, W.; Mulchandani, A.; Yan, Y. *Angew. Chem. Int. Ed.* **2005**, *44*, 6009.
(7) Jin, M.; Feng, X.; Feng, L.; Sun, T.; Zhai, J.; Li, T.; Jiang, L. *Adv. Mater.* **2005**, *17*, 1977.
(8) Xie, Q.; Xu, J.; Feng, L.; Jiang, L.; Tang, W.; Luo, X.; Han, C. C. *Adv. Mater.* **2004**, *16*, 302.
(9) Luo, Z.; Zhang, Z.; Hu, L.; Liu, W.; Guo, Z.; Zhang, H.; Wang, W. *Adv. Mater.* **2008**, *20*, 970.
(10) Gu, Z. Z.; Uetsuka, H.; Takahashi, K.; Nakajima, R.; Onishi, H.; Fujishima, A.; Sato, O. *Angew. Chem. Int. Ed.* **2003**, *42*, 894.
(11) Wu, Z.; Lee, D.; Rubner, M. F.; Cohen, R. E. *Small* **2007**, *8*, 1445.
(12) Li, Y.; Zhang, J.; Zhu, S.; Dong, H.; Jia, F.; Wang, Z.; Sun, Z.; Zhang, L.; Li, Y.; Li, H.; Xu, W.; Yang, B. *Adv. Mater.* **2009**, *21*, 4731.
(13) Min, W. L.; Jiang, B.; Jiang, P. *Adv. Mater.* **2008**, *20*, 3914.
(14) Zhao, B.; Moore, J. S.; Beebe, D. J. *Science* **2001**, *291*, 1023.
(15) Gau, H.; Herminghaus, S.; Lenz, P.; Lipowsky, R. *Science* **1999**, *283*, 46.
(16) Higgins, A. M.; Jones, R. A. L. *Nature* **2000**, *404*, 476.
(17) Xia, D. Y.; Brueck, S. R. J. *Nano Lett.* **2008**, *8*, 2819.
(18) Vorobyev, A. Y.; Guo, C. L. *Appl. Phys. Lett.* **2009**, *94*, 224102.
(19) Morita, M.; Koga, T.; Otsuka, H.; Takahara, A. *Langmuir* **2005**, *21*, 911.
(20) Sommers, A. D.; Jacobi, A. M. *J. Micromech. Microeng.* **2006**, *16*, 1571.
(21) Chung, J. Y.; Youngblood, J. P.; Stafford, C. M. *Soft Matter* **2007**, *3*, 1163.
(22) Wu, H.; Zhang, R.; Sun, Y.; Lin, D. D.; Sun, Z. Q.; Pan, W.; Downs, P. *Soft Matter* **2008**, *4*, 2429.
(23) Zhao, Y.; Lu, Q. H.; Li, M.; Li, X. *Langmuir* **2007**, *23*, 6212.
(24) Wu, D.; Chen, Q.; Yao, D. J.; Guan, Y. C.; Wang, J. N.; Niu, L. G.; Fang, H. H.; Sun, H. B. *Appl. Phys. Lett.* **2010**, *96*, 053704.
(25) Chen, Y.; He, B.; Lee, J.; Patankar, N. A. *J. Colloid Interface Sci.* **2005**, *281*, 458.

devices and nanopatterns.[14−16] Fortunately, multiscale microstructures[26] were first prepared by imprint lithography to investigate anisotropic wetting along both directions. The parallel contact angle on hierarchal structures without modification reached as much as 113°. This demonstrated the advantage of hierarchal structures for mimicking natural anisotropic surfaces. However, this method possessed a complex and expensive fabrication process. Moreover, how to precisely control anisotropic wetting with two directions by hierarchical microstructures for wmimicking natural anisotropic wetting remains untouched. Therefore, it is highly desired to exploit a simple approach for preparing hierarchical microstructures and precisely controlling anisotropic wetting along two directions.

Multibeam laser interference lithography[27] is a promising and maskless technique, which has been used to fabricate periodic microstructures such as one-dimensional (1D) grating, two-dimensional (2D) pillar arrays,[28] and three-dimensional (3D) photonic crystals.[29] However, there are few reports about multiscale micro/nanostructures by this approach. In this paper, we present a kind of improved laser interference lithography, based on intensity-modulated multibeams to realize special microstructures, which appear to resemble an array of a string of pearls. Due to their different height change along the perpendicular and parallel directions, these micropearl arrays were used to control two-direction CAs. Then, by precise design of the shape and size of the pearls, controlled anisotropic biosurfaces were prepared. This method is simple, rapid, and cost-effective. Moreover, this method is highly designable. By appropriate design and surface modification, natural anisotropic surfaces with two different CAs ($146° \pm 2°/153° \pm 3°$) were precisely mimicked by our biomimetic anisotropic surface with the CAs $145° \pm 1°/150° \pm 2°$.

Experimental Section

The Preparation of Micropearl Arrays. The photoresist (Norland: NOA 61) was diluted with acetone with the volume ratio 1:1. The resin was spin-coated on a glass slide cleaned with acetone and absolute ethanol at different rotation speeds to obtain the needed thickness of the resin. A frequency-tripled, Q-switched, single-mode Nd:YAG laser (Spectra-physics) with about 10 ns pulse width was used for laser interference. The improved interference lithography was based on intensity modulation of four beams (inset of Figure 1c). The intensity of beams 1 and 3 was the same. The intensity of beam 2 was equal to that of beam 4, while the intensity of beams 2 and 4 was far lower than that of beams 1 and 3. The four beams were overlapped on the sample to produce designed interference patterns. After irradiation, micropearl arrays were formed. Then the samples were developed in acetone for 1 min to remove the unpolymerized resin, and the needed micro/nanostructures were left. The low surface energy modification material was a fluoroalkysilane ($CF_3(CF_2)_5$-$CH_2CH_2SiCl_3$), which was evaporated for 2 h at 60 °C, to enhance the hydrophobic ability of micropearl arrays.

Sample Characterization. The morphologies of the micropearl arrays were characterized by using a field emission scanning electron microscope (SEM, JSM-7500F, JEOL, Japan). The contact angle measurements were made using a Contact Angle System OCA 20 instrument (DataPhysics Instruments GmbH, Germany) at ambient temperature. The static contact angles were measured by the sessile drop method with a water drop (3 μL).

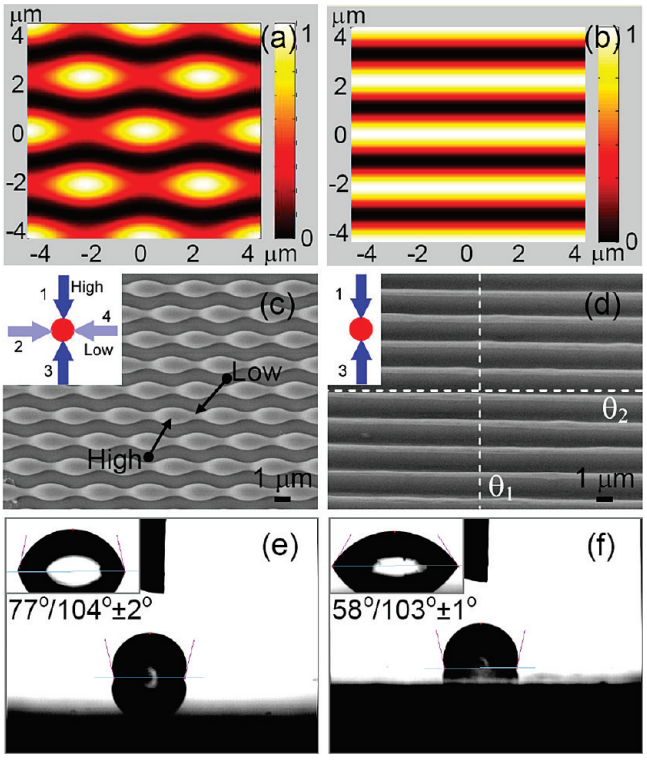

Figure 1. Micropearl arrays fabricated by improved laser interference lithography. (a,b) Calculated intensity distributions of modified four-beam and common two-beam interference lithography. (c,d) SEM images of micropearl arrays and grooved structures prepared by improved four-beam and common two-beam interference lithography. (e,f) CA measurement showing that θ_2 was enhanced by height variations Δh of micropearl arrays while θ_1 determined by the resin thickness kept constant.

Results and Discussion

Improved Interference Lithography for Preparing Micropearl Array Microstructures. Shown in Figure 1c is a bird-view SEM image of regular micropearl arrays fabricated by modified interference lithography. This kind of special microstructure consists of a high region h_1 and low one h_2 (two arrows in Figure 1c). The area of the sample determined by the size of laser beams is about 60 mm^2. For comparison, common grooves (Figure 1d) were fabricated by two-beam (the inset of Figure 1d) laser interference lithography. The contact angles along various directions are different on anisotropic microstructures, but there is a minimal and maximal value. The contact angle θ_1 along the parallel direction is the minimal value, while the contact angle θ_2 is the maximal value along the perpendicular direction. So, the perpendicular and parallel contact angles were measured to characterize the anisotropy degree of the microstructure surface. For single level grooved structures, the height variations along the perpendicular direction were determined by the groove height while there were no height variations along the parallel direction. So, the perpendicular CA θ_1 could be changed by adjusting the thickness of the resin while the parallel CA θ_2 was difficult to control because the CA depended strongly on the groove height and weakly on the other parameters[24] in the common microfabrication scale, about the magnitude of several micrometers. For this reason, our concept is to introduce the height variations along the parallel directions ($\Delta h = h_1 - h_2$). Although four-beam interference lithography could be used to realize pillar arrays with Δh, pillar arrays were isotropic and θ_1 was equal to θ_2. Here, a kind of modified laser interference lithography was proposed, as shown in

(26) Zhang, F. X.; Low, H. Y. *Langmuir* **2007**, *23*, 7793.
(27) Wu, D.; Chen, Q. D.; Xu, B. B.; Jiao, J.; Xu, Y.; Xia, H.; Sun, H. B. *Appl. Phys. Lett.* **2009**, *95*, 091902.
(28) Sun, H. B.; Nakamura, A.; Shoji, S.; Duan, X. M.; Kawata, S. *Adv. Mater.* **2003**, *15*, 2011.
(29) Kondo, T.; Matsuo, S.; Juodkazis, S.; Misawa, H. *Appl. Phys. Lett.* **2001**, *79*, 725.

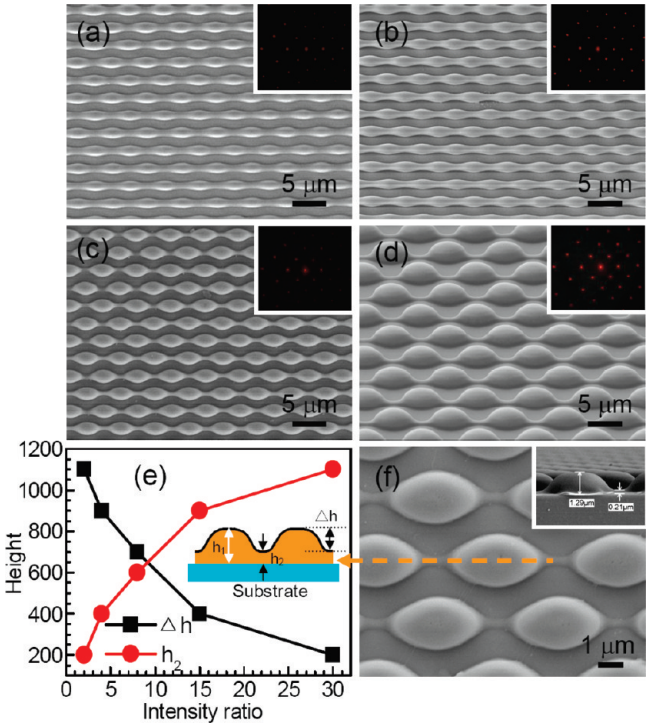

Figure 2. Relationship between Δh and intensity ratio. (a−d) SEM images of various micropearl arrays prepared by different intensity ratios. (a−c) Bird's eye view SEM image and (d) 45°-tilted view SEM image. The insets are the optical diffraction patterns of regular micropearl arrays under 632-nm laser illumination. (e) Strong dependence curve between Δh, h_2 and the intensity ratio. h_2 dramatically increased and Δh decreased as the intensity ratio increased, which agreed well with the theoretical results. (f) Magnified bird's eye view SEM image of (d). The inset is its 90°-tilted SEM image.

the inset of Figure 1c. For two-beam interference lithography, beam 1 and beam 3 (the inset of Figure 1d) were used. By adding another two beams 2 and 4 with lower laser intensity (the inset of Figure 1c), the height variations were introduced along the parallel direction. According to theoretical calculation (Supporting Information section 1), the laser intensity distribution for this modified four-beam interference lithography shown in Figure 1a is when the ratio of laser intensity between beams 1, 3 and beams 2, 4 was about 8:1. We found that the intensity distribution along the parallel direction had periodic variations while the one for two-beam interference lithography (Supporting Information section 2) kept constant (Figure 1b). Then, with this improved method, micropearl arrays (Figure 1c) were fabricated in the resin NOA 61, which agreed well with the theoretical interference patterns. The measured θ_1 and θ_2 values were 104° ± 2° and 77° ± 2° (Figure 1e) while they were 103° ± 2° and 58° ± 1° (Figure 1f) for the common groove structure (Figure 1d). θ_2 increased from 58° ± 1° to 77° ± 2° by these micropearl arrays, while there was no obvious difference in θ_1 which was determined by the thickness of the resin. The increase of θ_2 was mainly caused by the energy barrier[21,23] exerted by the Δh of micropearl arrays.

Various Micropearl Arrays by Different Laser Ratios. To systemically investigate anisotropic wetting, different micropearl arrays were prepared. Because h_2 and Δh depended on beams 2 and 4, different h_2 and Δh values could be realized by changing the ratio of laser intensity between 1, 3 and 2, 4. Shown in Figure 2a−d are various micropearl arrays fabricated with different intensity ratios 30:1, 15:1, 4:1, and 2:1, respectively. These four panels contain insets showing different optical diffraction patterns of

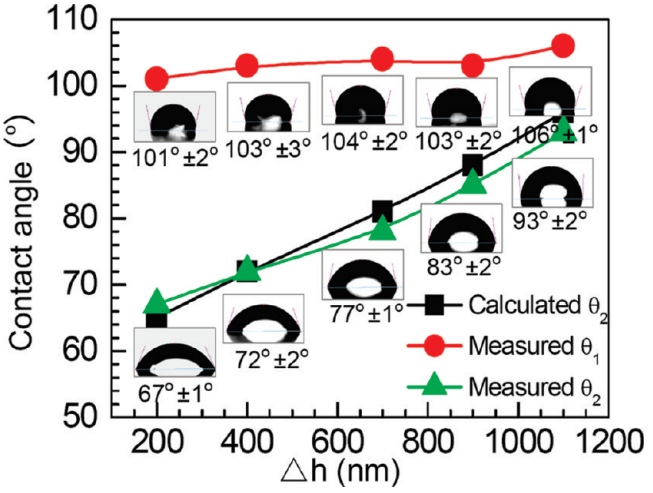

Figure 3. Strong dependence curve between Δh and the contact angle θ_2. θ_2 dramatically increased as Δh increased, which agreed well with the theoretical results based on a thermodynamic model.

various micropearl arrays under 632 nm laser illumination, showing anisotropic optical properties caused by these anisotropic micropearl arrays. When the intensity of beams 2 and 4 decreased (beams 1, 3/beams 2, 4 = 2:1), the fabricated structures (Figure 2d) were similar to spot arrays. From the magnified SEM image (Figure 2f), we could see that the thin line was very low. Its height was about 200 nm, according to the measurement from the 90°-tilted cross-sectional SEM image (the inset of Figure 2f). Δh was about 1.1 μm which was very close to the thickness of the resin (~1.3 μm). In contrast, when the intensity of beams 2 and 4 decreased (beams 1, 3/beams 2, 4 = 4:1, 8:1, and 15:1), h_2 increased to 400, 600, and 900 nm, and Δh decreased to 900, 700, and 400 nm, respectively. When the intensity of beams 2,4 was only 1/30 of the intensity of beams 1,3, the fabricated structures (Figure 2a) were more approximate to groove structures. h_2 reached as much as 1.1 μm, and Δh was only ~200 nm. From the dependence curve (Figure 2e) between Δh, h_2 and the intensity ratio, it was seen that h_2 dramatically increased and Δh decreased when the intensity ratio became big. This agreed well with the theoretical calculation of laser interference patterns.

The Relationship between θ_2 and Δh. According to CA measurements, θ_2 increased to 93° ± 2°, a little smaller than θ_1 (106° ± 1°) (Figure 3) when h_2 became small (~200 nm). This was because Δh increased to 1.1 μm when h_2 decreased. The increase of Δh leads to an increase of the energy barrier and the CA. In contrast, θ_2 decreased to 67° ± 1° when Δh was only ~200 nm caused by the increase of the laser intensity ratio. From the dependence curve between Δh and CAs, it was seen that θ_2 (the green triangle of Figure 3) dramatically increased as Δh became big while θ_1 (the red dot of Figure 3) kept constant. This agreed well with the theoretical calculation of the equilibrium CAs (the black square of Figure 3) by a thermodynamic model analysis.[24,30,31] In this model, it was considered that a system between a surface microstructure and water drop formed when the free energy (FE) was the least. First, along the corresponding surface geometrical configuration, the relative FE barrier between adjacent microstructures could be calculated. Then, the whole FE barrier was obtained (Supporting Information section 3). Along the relationship, the curve of FE and CA was calculated and the CA of the minimum FE was considered as the equilibrium CA

(30) Li, W.; Fang, G. P.; Li, Y. F.; Qiao, G. J. *J. Phys. Chem. B* **2008**, *112*, 7234.
(31) Li, W.; Amirfazli, A. *J. Colloid Interface Sci.* **2005**, *292*, 195.

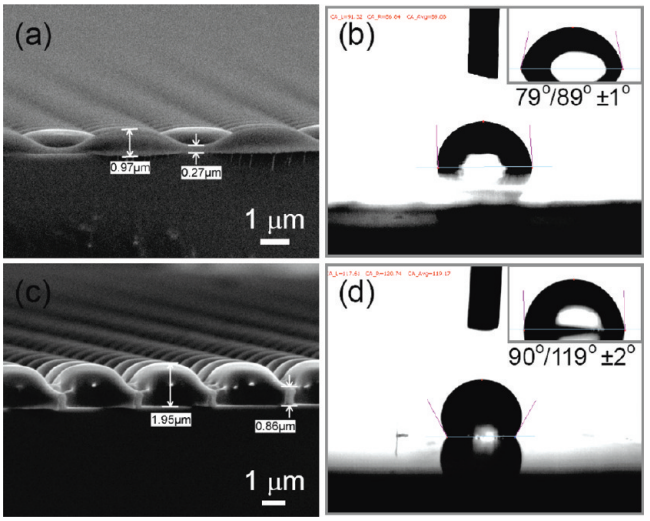

Figure 4. Controlled anisotropic surfaces with both directions by adjusting the thickness of the resin and the ratio of laser intensity. (a) Micropearl arrays with h_2/h_1 = 270 nm/970 nm, which is very close to the needed heights 300 nm/1 μm. (b) Measured θ_2 and θ_1 values were 79°/89° ± 1°, just as what we expect (80°/90°). (c) 90°-tilted SEM image of micropearl arrays with 0.86 μm/1.95 μm. (d) Measured CAs 90°/119° ± 2°, which agreed well with the designed value 90°/120°.

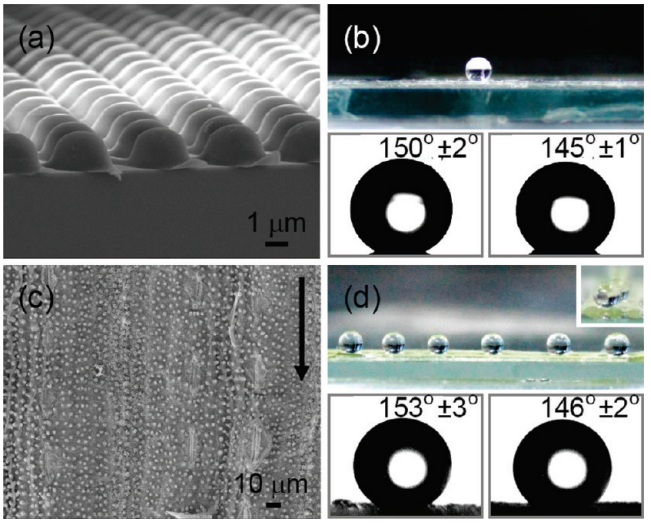

Figure 5. Comparison of biomimetic anisotropic surfaces and natural rice leaf. (a) Cross-sectional SEM image of micropearl arrays with height variations 1.75 μm/2 μm. (b) The upper figure is the digital photo of a water droplet on modified micropearl arrays. The lower figure is the measured CAs enhanced by fluoroalkysilane modification. (c) SEM image of natural rice leaf. (d) Digital photos of a water droplet on the rice leaf along both directions and the CA measurement showing that the designed anisotropy (145° ± 1°/150° ± 2°) is close to those natural one (146° ± 2°/153° ± 3°).

because a system with the smallest FE was steadiest. The wetting in our case is in the noncomposite state, where the water penetrates into the micropearl arrays, because θ_2 strongly depends on the height. When a water droplet spreads along the parallel direction, it has to overcome the energy barrier caused by the height variations Δh. The greater the height variations, the bigger the energy barrier and θ_2. This makes it possible for us to precisely control θ_2 by this improved method. Hence, the anisotropic wetting properties along both directions (θ_1 and θ_2) could be controlled by the height variations Δh and the resin thickness which were adjusted by the ratio of laser intensity and the rotation speed of spin-coating, respectively.

Controlled Anisotropic Wetting along Two Directions. To verify this possibility, a certain anisotropic value, for example, 80°/90°, was freely chosen. According to the theoretical curve in Figure 3, h_2 would be 300 nm and h_1 should be 1 μm,[24] respectively. Experimentally, first a layer of 1 μm thickness resin was obtained by controlling the rotation speed. Then, by optimal laser intensity ratio (beams 1, 3 and beams 2, 4 = 3.5:1), regular micropearl arrays were prepared, as shown in Figure 4a. h_1 and h_2 were about 270 and 970 nm, respectively. The measured θ_2 and θ_1 values were 79°/89° ± 1° (Figure 4b), just as what we expected. To further verify the possibility of realizing controlled anisotropy with two directions, another anisotropic value, e.g., 90°/120°, would be obtained when h_1 and h_2 were about 0.9 and 2 μm, respectively, according to the theoretical analysis. By controlling the thickness of the resin and the ratio of laser intensity, regular micropearl arrays with height 0.86 and 1.95 μm (Figure 4c) were obtained. The measured θ_2 and θ_1 values were 90°/119° ± 2° (Figure 4d), which was approximate to the needed anisotropic value.

Comparison of Biomimetic Anisotropic Surfaces and Natural Rice Leaf. The rice leaf was one of the most typical examples for anisotropic wetting caused by those directional microstructures (Figure 5c). According to the CA measurements, θ_2 and θ_1 were about 146° ± 2° and 153° ± 3° (Figure 5d), respectively. The difference between both of the CAs was not big (~7°), but both θ_2 and θ_1 were very large because a large CA was beneficial to control the movement of the water droplet. The upper digital photo in Figure 5d also shows that the water droplet was nearly spherical along both directions and the difference was very small. However, most artificial anisotropic biosurfaces[19−23] reported before exhibited lower CAs (50°−130°). Here, in order to realize the anisotropic wetting of the rice leaf, we combined optimal micropearl arrays and low surface energy modification[5−13,32,33] which could increase the CAs. According to theoretical calculation, micropearl arrays with height variations 1.75 and 2 μm (Figure 5a) were prepared. After fluoroalkysilane modification, both θ_2 and θ_1 were dramatically enhanced, as shown in the digital photo of Figure 5b. θ_2 increased from 112° ± 2° to 145° ± 1°, and θ_1 was enhanced from 120° ± 3° to 150° ± 2°, which were very close to the anisotropic wetting of the rice leaf. However, the parallel θ_2 for common single level grooved microstructures by surface modification was only about 110°.[24]

Conclusion

We proposed a kind of improved interference lithography to realize large-area micropearl arrays for controlling anisotropic wetting along two directions. The relationship between anisotropy and parameter was systemically investigated. Then, both θ_1 and θ_2 of anisotropic surfaces could be freely designed and precisely realized by adjusting the thickness of the resin and the intensity ratio of four laser beams. Moreover, by combining appropriate parameters and low surface energy modification, θ_2 and θ_1 were further enhanced to 145° ± 1°/150° ± 2°, which made biomimetic anisotropic surfaces be more close to those natural ones. This method is simple, time-effective, and highly designable. These controlled biosurfaces will find broader

(32) Wu, D.; Chen, Q. D.; Xia, H.; Jiao, J.; Xu, B. B.; Lin, X. F.; Xu, Y.; Sun, H. B. *Soft Matter* **2010**, *6*, 263.
(33) Zhai, L.; Berg, M. C.; Cebeci, F. C.; Kim, Y.; Milwid, J. M.; Rubner, M. F.; Cohen, R. E. *Nano Lett.* **2006**, *6*, 1213.

applications in microfluidic devices, liquid transfer, and bioinspired systems.

Acknowledgment. The authors gratefully acknowledge support from the NSFC under Grant Nos. 90923037, 60978062, and 60525412.

Supporting Information Available: Additional figures and equations for improved four-beam laser interference lithography, two-beam laser interference lithography, and energy barrier calculation of a thermodynamic model. This material is available free of charge via the Internet at http://pubs.acs.org.